Surface Science 659 (2017) 9–15

Contents lists available at ScienceDirect

Surface Science

journal homepage: www.elsevier.com/locate/susc

Quantifying the delocalization of surface and bulk *F*-centers

Benjamin G. Janesko*, Stephanie I. Jones

Department of Chemistry and Biochemistry, Texas Christian University, Fort Worth, TX 76129, USA

A R T I C L E I N F O

Keywords:
Surface *F*-center
Delocalization
Electronic structure

A B S T R A C T

Electrons trapped in ionic crystal defects form color centers (*F*-centers) important in surface science, catalysis, and optoelectronic devices. We apply the electron delocalization range function (EDR) to quantify the delocalization of surface and bulk *F*-centers. The EDR uses computed one-particle density matrices to quantify "delocalization lengths" capturing the characteristic size of orbital lobes. *Ab initio* cluster model calculations confirm that the delocalization lengths of bulk alkali halide *F*-centers scale with the size of the anion vacancy. Calculations on magnesium oxide surface F_s and F_s^+ centers, as well as other anionic surface defects, show how the trapped electrons' delocalization depends on the defect morphology, defect occupancy, and the approximate treatment of electron correlation. Application to N_2 activation by anionic surface defects illustrate how the trapped electron localizes into the adsorbed molecule's unoccupied orbitals. The results confirm that the EDR provides a useful tool for understanding the chemistry of surface- and bulk-trapped electrons.

1. Introduction

F-centers in alkali halides and alkaline-earth oxides have been studied for many decades [1–9]. F (*Farbe*) centers are defects in ionic crystals in which an anion is replaced by one or more trapped electrons. Confined and shielded by the surrounding crystal lattice, these trapped electrons form gap states possessing unique optical, electric, and magnetic properties [10,11] relevant to optoelectronic devices [12–16]. *F*-centers at surfaces, along with other anionic defects, are also relevant in catalysis [17–23].

In this work, we use electronic structure calculations to study the quantum-mechanical localization of electrons trapped in surface and bulk *F*-centers [24,25]. Electronic structure calculations simulating surface and bulk *F*-centers have a long history [7,26,27]. Modern simulations typically treat either a single *F*-center surrounded by a finite cluster of nearby atoms [28–30,19–21,31], or an infinite, periodic array of more or less distant *F*-centers [32,33,23]. Many of these simulations target energetic properties such as ionization or excitation energies. These properties can be quite sensitive to technical details of the simulation [33]. Fewer simulations consider our focus, the structure and localization of the trapped electrons. Previous studies of trapped electrons' localization consider either the single (highest occupied) orbital containing the trapped electron, [34–36] or the spin polarization of the electron density [25]. Both approaches have limitations. Focus on single orbitals can be problematic for systems with "strong coupling", where molecular orbital theory breaks down [37,38]. Analyses of spin polarization are not applicable to closed-shell systems, such as two singlet-coupled electrons trapped in a single defect. Bader and Platts went beyond these limitations, using the quantum theory of atoms in molecules [39] to characterize bulk *F*-centers in LiF [31]. Calculations on a simple $Li_{14}F_{12}^+$ cluster model confirmed that the trapped electron yields a "non-nuclear attractor", a maximum in the electron density occurring not at a nucleus, but at the defect center. Non-nuclear attractors were also found in sodium electrosodalite [40] and magnesium oxide [41] *F*-centers. The electron localization function [42] also gives insight into *F*-centers [32]. However, none of these methods directly quantify the trapped electrons' "size", i.e., the quantum-mechanical delocalization length.

We recently proposed the electron delocalization range function $\mathrm{EDR}(\vec{r}; d)$ to quantify and visualize aspects of electron delocalization [43]. The EDR quantifies the degree to which the one-particle density matrix

$$\gamma(\vec{r}, \vec{r}') = N\int d^3\vec{r}_2 \ldots \int d^3\vec{r}_N \Psi(\vec{r}, \vec{r}_2 \ldots \vec{r}_N)\Psi^*(\vec{r}', \vec{r}_2 \ldots \vec{r}_N) \quad (1)$$

of calculated N-electron wavefunction Ψ "delocalizes" distance d about point $\vec{r}$. The EDR does this by projecting the density matrix onto a model density matrix γ_{mod} which decays by construction over distance d:

$$\mathrm{EDR}(\vec{r}; d) = \rho^{-1/2}(\vec{r}) \int d^3\vec{r}' \gamma(\vec{r}, \vec{r}')\gamma_{mod}(\vec{r} - \vec{r}', d) \quad (2)$$

$$\gamma_{mod}(u, d) = \left(\frac{2}{\pi d^2}\right)^{3/4} \rho^{1/2}(\vec{r}) \exp(-\frac{u^2}{d^2}) \quad (3)$$

---

* Corresponding author.
E-mail address: b.janesko@tcu.edu (B.G. Janesko).

http://dx.doi.org/10.1016/j.susc.2017.01.005
Received 7 December 2016; Received in revised form 13 January 2017; Accepted 15 January 2017

The prefactors in Eq. (3) ensure that γ_{mod} has the proper units and normalization $\int d^3\vec{r}'|\gamma(\vec{r},\vec{r}')|^2 = \rho(\vec{r})$. The unitless EDR obeys $|\text{EDR}(\vec{r};d)|^2 \leq 1$ by the Cauchy-Schwarz inequality. Distance $D(\vec{r}) = \text{argmax}_d \text{EDR}(\vec{r};d)$ maximizing $\text{EDR}(\vec{r};d)$ at point $\vec{r}$ serves as a "characteristic delocalization length" of electrons at $\vec{r}$. The EDR is inspired by our [44] and others' [45–47] work quantifying delocalization of the one-particle density matrix and exchange hole. The EDR approximately quantifies the radius of the *orbital lobes* dominating in region $\vec{r}$: for example, comparisons of the bonding and antibonding states of H_2^+ show that $D(\vec{r})$ is relatively large in the single lobe of the bonding orbital, and relatively small in each of the two lobes of the antibonding orbital [48]. (We use "orbital lobe" language as an aid to understanding, not because the EDR is in some way "orbital dependent". As a function of the full one-particle density matrix, the EDR is independent of unitary transforms of the occupied orbital space, and can readily be evaluated for multiconfigurational and multireference wavefunctions.) Our earliest study of the EDR considered a crude periodic supercell model of bulk NaCl *F*-centers. Points $\vec{r}$ in the defect site had $\text{EDR}(\vec{r};d)$ maxima shifted to large d [43].

The EDR provides a "characteristic delocalization length" D_{max} of an N-electron system's most weakly bound electron, defined as

$$D_{max} = \underset{d}{\text{argmax}} \langle \text{EDR}(d)\rangle_N - \langle \text{EDR}(d)\rangle_{N-1} \tag{4}$$

$$\langle \text{EDR}(d)\rangle_N = \int d^3\vec{r}\rho(\vec{r})\text{EDR}(\vec{r};d) \tag{5}$$

Here $\langle \text{EDR}(d)\rangle_N$ is the system-averaged EDR of an N-electron system, which is compared to the system average with N-1 electrons. The corresponding difference in total energies defines the vertical detachment energy (VDE). D_{max} of anionic water clusters, evaluated from Hartree-Fock calculations, has a one-to-one relationship with a very different measure of electron radius, the radius of gyration of the singly occupied molecular orbital [49,35]. Real-space plots of $\text{EDR}(\vec{r};D_{max})$ characterize the region of space occupied by the trapped electron, highlighting the major lobe of the singly occupied orbital. Evaluating the EDR from correlated wavefunctions quantifies the effects of "strong" correlation on the electron distribution [49,50]. Our most recent study used D_{max} to quantify strong correlation in coupled *F*-center defects, which we showed map onto the "textbook" problem of strong correlation in stretched H_2 [51].

Here we significantly extend Ref. [51] by applying the EDR to surface and bulk *F*-centers and other anionic defects. Our results confirm that the EDR is a practical tool for building insight into trapped electrons. We find that in alkali halide bulk *F*-centers, the trapped electrons' D_{max} scales with the size of the cavity. Calculations on surface *F*-centers and other surface defects on magnesium oxide confirm the relatively large delocalization of electrons trapped at surface defects. Application to N_2 activation by surface trapped electrons [28] illustrate how the trapped electron localizes onto the absorbed molecule.

2. Computational methods

Calculations use the development version of the Gaussian suite of programs [52]. Calculations use Hartree-Fock theory (HF), second-order many-body perturbation theory (MP2), and generalized Kohn-Sham density functional theory (DFT) [53,54]. DFT calculations use several density functional approximations (DFAs) for the exact exchange-correlation functional: the local spin-density approximation (LSDA) [55], the Perdew-Burke-Ernzerhof generalized gradient approximation (PBE GGA) [56], and Becke's three-parameter global hybrid incorporating Lee-Yang-Parr correlation (B3LYP) [57–59]. Most calculations use the 6-31+G(d) atom-centered basis set, freeze the atomic positions to those of the experimental defect-free bulk cubic lattice, and place "ghost" atom basis functions at the defect center. Calculations on open-shell systems are performed spin-unrestricted. The EDR and D_{max} are evaluated as described previously [43]. Calculations on the particle-in-a-box model use a Mathematical worksheet provided as Supporting Information. Calculations comparing ground and excited states use the experimental lattice parameters and embed the clusters in >100 effective core potentials and >1000 point charges to simulate the surrounding ionic lattice. As in Ref. [51], we simulate Li^+ and F^- as point charges +1 and −1 surrounded by the SBKJC [60] large-core effective core potentials for Li^+ and Na^+, respectively.

Table 1
Cavity radius *L* and delocalization length D_{max} of bulk alkali halide *F*-centers.

Property	LiF	NaCl	KBr
Cavity radius *L* (Bohr, Ref. [61]	3.81	5.33	6.23
D_{max} (bohr), Eq. (6)	3.22	4.50	5.26
D_{max} (bohr), cluster model	2.81	4.08	4.47

3. Results and discussion

3.1. Bulk F-centers

Before considering surface *F*-centers, we confirm that the EDR gives reasonable results for bulk *F*-centers. Table 1 reports D_{max} evaluated for isolated paramagnetic bulk *F*-centers in alkali halides. D_{max} is compared to the cavity radius *L*, defined as the nearest-neighbor distance of the defect-free crystal at 0 K [61]. D_{max} is evaluated for the cluster model in Fig. 1, and for a much simpler model [62]: a single electron in a cubic box of side length 2*L*. Numerical evaluation yields the linear relation

$$D_{max} = 0.845L \tag{6}$$

(Supporting Information). This physically realistic result shows that the trapped electron's characteristic radius D_{max} is somewhat less than the cavity radius *L*. The more realistic *ab initio* cluster model gives a somewhat smaller D_{max}, consistent with Pauli repulsion from the cavity wall. Fig. 1 shows that $\text{EDR}(\vec{r};D_{max})$ highlights the major lobe of the electron spin density, consistent with the EDR from electrons trapped in solvent clusters [49] and electrides [50].

Bare clusters like those in Fig. 1 provide a rather poor model of the energetics of *F*-center defects [33]. We thus investigate how well the bare cluster models the defect electronic structure, comparing electrostatic embedding's effects on VDE vs. D_{max}. Table 2 reports the VDE and D_{max} of an isolated bulk paramagnetic *F*-center in NaCl, evaluated for a $Na_{14}Cl_{13}^+$ cluster embedded in N_{PC} shells of point charges. (We choose even N_{PC} to ensure a total cluster charge +1). Electrostatic embedding has a dramatic effect on the VDE, but a negligible effect on D_{max}, confirming that confinement is largely a function of the first shell of surrounding ions.

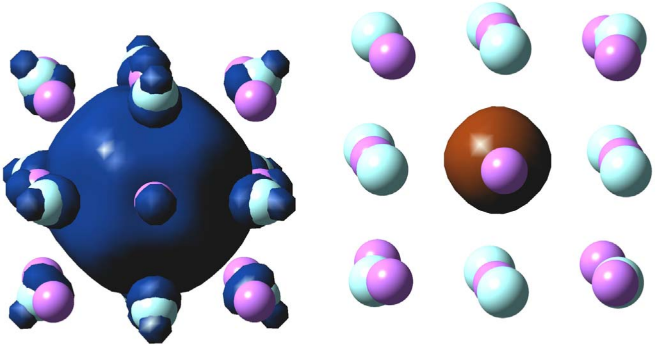

Fig. 1. Isosurfaces of spin density (left) and $\text{EDR}(\vec{r};D_{max})$ (right) for a cluster model of an isolated bulk LiF *F*-center.